J Fluoresc (2017) 27:235–242
DOI 10.1007/s10895-016-1950-9

ORIGINAL ARTICLE

The Effect of Substituent Position on Excited State Intramolecular Proton Transfer in Benzoxazinone Derivatives: Experiment and DFT Calculation

Gao-Feng Bian[1,2] · Yun Guo[1] · Xiao-Jing Lv[1] · Cheng Zhang[1]

Received: 23 July 2016 / Accepted: 3 October 2016 / Published online: 18 October 2016

Abstract The preparation and the photophysical behaviour of two benzoxazinone derivatives isomers 2-(1-hydroxynaphthalen-2-yl)-4H-benzo[e][1, 3]oxazin-4-one(**1**) and 2-(3-hydroxynaphthalen-2-yl)-4H-benzo[e][1, 3]oxazin-4-one(**2**) designed for displaying were reported. The effect of substituent position and solvent effect on the excited state intramolecular proton transfer (ESIPT) dynamics and the spectroscopic properties were investigated using a combined theoretical (i.e., time-dependent density function theory (DFT)) and experimental (i.e., steady-state absorption and emission spectra and time-resolved fluorescence spectra) study. The results showed that compound **1** would facilitate ESIPT process and favored the keto tautomer emission, while compound **2** suppressed the ESIPT process and favored the enol emission.

Keywords Benzoxazinone · ESIPT · DFT calculation · Time-resolved fluorescence spectra · Solvent effect

Introduction

Excited state intramolecular proton transfer (ESIPT) has been extensively studied in chemistry and biology [1, 2]. This has aroused experimental and theoretical interest in the mechanism insights of ESIPT [3, 4]. In a typical ESIPT process, photo excitation prompts the proton migration from a donor atom (e.g.-OH) to adjacent acceptor atom (e.g. N, S, O), resulting in the tautomers. Usually, ESIPT involves a four-level circle reaction: the ground state of enol (E) → the excited state of enol (E*) → the excited state of keto (K*) → the ground state of keto (K) → E. Consequently, ESIPT chromophores often exhibit a dual emission due to the excited enol form (E*) and the excited keto form (K*), which induces an abnormally large Stokes shift without self-absorption. These unique characters have attracted enormous attentions for their potential applications, such as laser dyes [5], ultraviolet photostabilizer [6], radiation scintillators [1], organic electroluminescent optical materials [7], fluorescence probe [8] and so on.

Since the first observation of ESIPT in salicylic acid have been reported by Weller [9], various ESIPT molecules have been obtained, such as benzophenones [10], hydroxyflavones [11], anthraquinones [12], pyridyls [13], quinolines [14], benzazoles [15, 16], azoles [17, 18], and salicylidene anilines [19]. The basics of ESIPT process have also received a great maturity through the massive volume of research works. Nevertheless, controlled synthesis and detailed mechanism is still a challenge due to its inherently complicated physical and chemical nature, such as the cleavage and formation of H-bond and nuclear rearrangement. At present, design and synthesis of new molecules and the detailed mechanism analysis are two main aspects for ESIPT research. Benzoxazinone derivatives have anti-platelet aggregation activity [20] and are used in medicines, pesticides and dyes. Compared with benzothiazoles which have been widely investigated in ESIPT, there is less relevant literature about ESIPT in this system. In this work, we designed and synthesized a new benzoxazinone derivative **1** and focused on its interesting

Electronic supplementary material The online version of this article (doi:10.1007/s10895-016-1950-9) contains supplementary material, which is available to authorized users.

✉ Cheng Zhang
czhang@zjut.edu.cn

[1] College of Chemical Engineering, Zhejiang University of Technology, Hangzhou 310014, People's Republic of China

[2] Key Laboratory of Organosilicon Chemistry and Material Technology, Hangzhou Normal University, Hangzhou 311121, People's Republic of China

ESIPT behaviors. And also, for comparison, another benzoxazinone derivative **2** which has already been synthesized by Geigy in 1970 [21] was also synthesized and investigated. It was isomer of compound **1**. Furthermore, a large volume of theoretical and experimental works have been done to gain more insight into the relationship for the photophysical behaviors versus structural properties.

Experimental

Material and General Methods

All reagents were obtained from commercial suppliers and used without further purification unless otherwise indicated. Glassware was dried in an oven at 100 °C and cooled under a stream of inert gas before use. The ^{1}H NMR was recorded on a Bruker AVANCE III 500 MHz instrument (Bruker, Switzerland) using dimethyl sulfoxide-d_6(DMSO-d_6) as the solvent. The UV-vis absorption spectrum was recorded on a Perkin Elmer Lambda 35 spectrophotometer. Fluorescent measurements were recorded on a Perkin-Elmer LS-55 luminescence spectrophotometer. ESI-MS spectra were obtained with an Agilent 6210 time-of-flight (TOF) mass spectrometer. All the solvents employed for the spectroscopic measurements were of UV spectroscopic grade (Aldrich).

Time-resolved fluorescence measurements were performed with the time-correlated single-photon counting (TCSPC) technique, and fitted to exponential functions with deconvolution of the measured instrument response function (IRF) using a FLS-980 Fluorescence Lifetime and Steady State Spectrometer with a sub-nanosecond pulsed LED (EPLED 320) as an excitation source. Fluorescence decay times were determined from the decays using the least-squares fitting method. The fitting was assumed to be correct when the goodness-of-fit value χ^2 was lower than 1.2.

Synthesis of 2-(1-hydroxynaphthalen-2-yl)-4H-benzo[e][1, 3]oxazin-4-one(1)

Salicylic acid (2 g, 14.5 mmol), 1-hydroxy-2-naphthamide (2.1 g, 11.1 mmol) and pyridine (1 mL) were refluxed in xylene (20 mL). Thionyl chloride (1.9 g, 16.0 mmol) was added with vigorous stirring over a period of 4 h. An intense evolution of SO_2 and HCl was noted and the precipitation was formed. The solution was continually stirred for an additional 30 min, and the xylene was removed by reduced-pressure distillation. The resulting solid residue was suspended in EtOH (30 mL) and acetic acid (1 mL). The mixture was heated gently and then allowed to cool to 20 °C. The precipitate was filtered and recrystallized from 2-methoxyethanol (35 mL). Yield: yellow solid (2.1 g, 7.2 mmol, 65 %).^{1}H NMR (DMSO-d_6, 500 MHz) δ(ppm) 14.810 (s, 1H), 8.398 (d, 1H, J = 8.0), 8.137 ~ 8.092 (m, 2H), 7.986 ~ 7.952 (m, 2H), 7.852 (d, 1H, J = 8.0), 7.768 (t, 1H, J = 8.0), 7.681 ~ 7.602 (m, 2H), 7.560 (d, 1H, J = 9.0). ^{13}C NMR ($CDCl_3$, 125 MHz): δ(ppm) 165.89, 163.91, 163.70, 154.19, 137.53, 135.46, 130.44, 127.90, 127.55, 126.98, 126.19, 125.37, 124.77, 122.32, 119.10, 118.3116.91, 103.99. HRMS: m/z Calcd for C18H11NO3, 289.0733; found, 312.0631[M + Na]$^+$.

Synthesis of 2-(3-hydroxynaphthalen-2-yl)-4H-benzo[e][1, 3]oxazin-4-one(2)

Salicylic acid (2 g, 14.5 mmol), 3-hydroxy-2-naphthamide (2.1 g, 11.1 mmol) and pyridine (1 mL) were refluxed in xylene (20 mL). Thionyl chloride (1.9 g, 16.0 mmol) was added with vigorous stirring over a period of 4 h. An intense evolution of SO_2 and HCl was noted and the precipitation was formed. The solution was continually stirred for an additional 30 min, and the xylene was removed by reduced-pressure distillation. The resulting solid residue was suspended in EtOH (30 mL) and acetic acid (1 mL). The mixture was heated gently and then allowed to cool to 20 °C. The precipitate was filtered and recrystallized from 2-methoxyethanol (35 mL). Yield: yellow solid (1.7 g, 5.9 mmol, 53 %). ^{1}H NMR (DMSO-d_6, 500 MHz): δ(ppm) 12.430 (d, 1H, J = 3.0), 9.00 (s, 1H), 8.155 ~ 8.041 (m, 2H), 7.998 (t, 1H, J = 8.5), 7.900 ~ 7.796 (m, 2H), 7.692 ~ 7.559 (m, 2H), 7.489 ~ 7.396 (m, 2H). ^{13}C NMR (DMSO-d_6, 101 MHz): δ(ppm) 164.99, 164.06, 156.48, 154.61, 138.09, 136.66, 132.49, 130.30, 129.85, 127.82, 127.35, 127.22, 126.57, 124.75, 118.39, 118.01, 114.58, 112.11. HRMS: m/z calcd for C18H11NO3, 289.0733; found, 312.0631[M + Na]$^+$ (Scheme 1).

Computational Details

All calculations were performed using density functional theory (DFT) calculations by help of Gaussian 09 software [22].

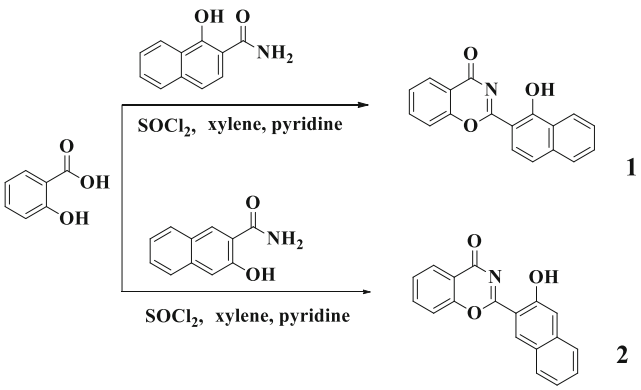

Scheme 1 Synthetic routes for preparation of the compound **1** and **2**

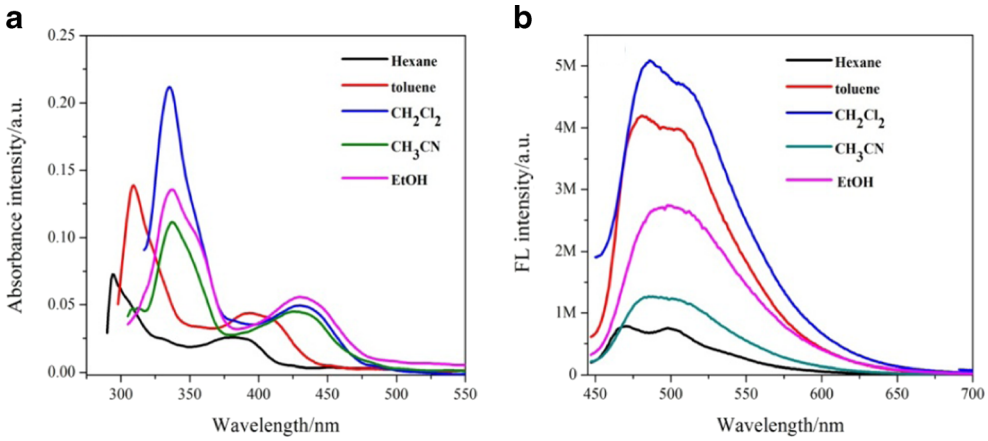

Fig. 1 **a** UV-vis absorption of **1** in different solutions. **b** Fluorescence emission spectra of **1** in different solutions. c = 1.0×10^{-5} M. λ_{ex} = 365 nm

Geometrical optimizations without any restrictions were conducted based on the level of CAM-B3LYP/6-31G**, where the dispersion correction of CAM algorithm was utilized to describe the weak interaction. Furthermore, the local stable states were further confirmed by frequency analysis. Potential energy surface (PES) for the ground state and the first excited state were scanned. In this process, the bond length of O-H were restricted in the range of 0.90–2.1 Å for **1** and 0.89–2.1 Å for **2**, while the remaining parts were fully relaxed. The optimization and PES of the first excited states were conducted by the method of time-dependent density functional theory (TD-DFT), where 80 exited states were considered. In the calculation, we took two solvents (dichloromethane and n-hexane) into account.

Results and Discussion

Steady-State Absorption and Emission Spectra

The UV-vis absorption spectra of compound **1** in different solvents were shown in Fig. 1a. The shape of the absorption spectra were almost similar in different solvents with different polarity, which exhibited a strong π-π* transition peak at about 290–340 nm and the second peak and broad band in the range of 400–500 nm. The solvent polarity exerted a significant effect on the absorption spectra and a red shift was observed with the increasing of the solvents polarity, probably due to the stabilizing interaction between the polar solvent molecular and compound **1**. Different to the absorption spectra, the emission spectra of **1** exhibited a slight red shift with the increasing of the solvents polarity and showed a single emission band at about 475 nm in all the solvents. And the Stokes shift in the range of 151–175 nm in different solvents could be observed. Hence, we assigned the only emission band to the keto emission. The presence of ESIPT phenomenon and intramolecular charge transfer (ICT) were maybe responsible for the large Stokes shift [23].

The UV-vis absorption spectra of the compound **2** were shown in Fig. 2a. Similar to compound **1**, the absorption spectra showed a strong π-π* transition with a maximum absorption at about 320–370 nm in different solvent and exhibited obvious red shift with the increasing polarity of the solvents, probably due to the stabilizing interaction between the polar solvent molecule and compound **2**. The shapes of emission spectra of **2** were totally different in various solvents (Fig. 2b). In n-hexane

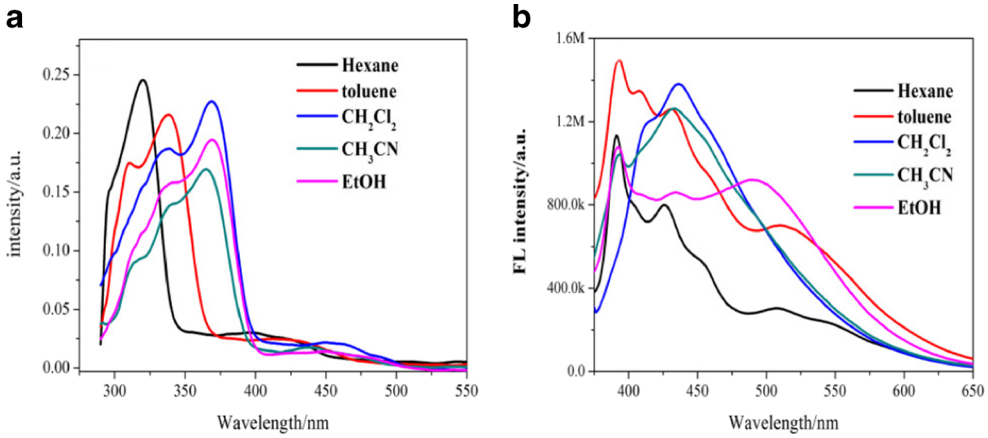

Fig. 2 **a** UV-vis absorption of **2** in different solutions. **b** Fluorescence emission spectra of **2** in different solutions. c = 1.0×10^{-5} M. λ_{ex} = 350 nm

and toluene, **2** showed two emission bands around 430 nm and 509 nm, respectively, and the longer emission bands could be attributed to the keto tautomer, produced by the ESIPT process. In polar solvents such as CH_2Cl_2 and CH_3CN, **2** showed a single emission band and the emission band at 509 nm disappeared, that is the keto emission disappeared. In protic polar solvent CH_3CH_2OH, the different emission was observed and a new emission peak at 490 nm appeared which may be originated from the solute-solvate interaction. These results suggested that **2** underwent the excited state intramolecular proton transfer in weak polarity solutions such as n-hexane and toluene, while in polar solvents such as CH_2Cl_2 and CH_3CN, ESIPT process was inhibited. The polarity parameters of the solvents used are summarized in Table S1.

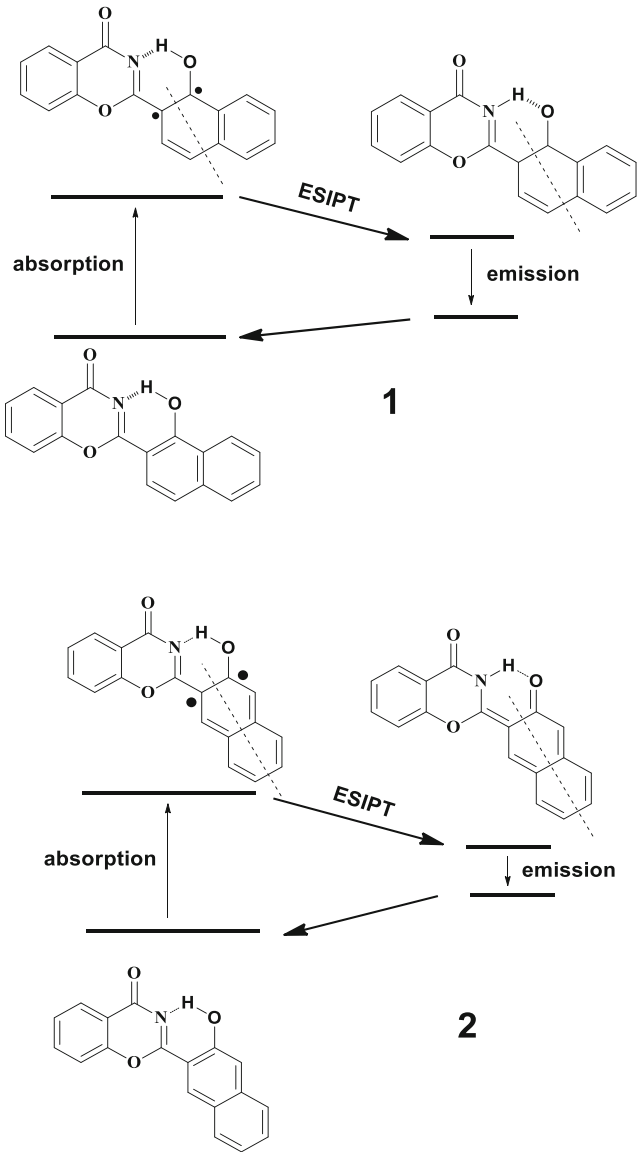

Fig. 3 Schematic diagrams for nodal plane models and ESIPT process of **1** and **2**

The difference in the Stokes shift of the ESIPT fluorescence between compound **1** and **2** could be explained in terms of nodal-plane model (Fig. 3) proposed by Nagaoka et al. [24, 25]. In compound **1**, the nodal plane lies on only one of the two

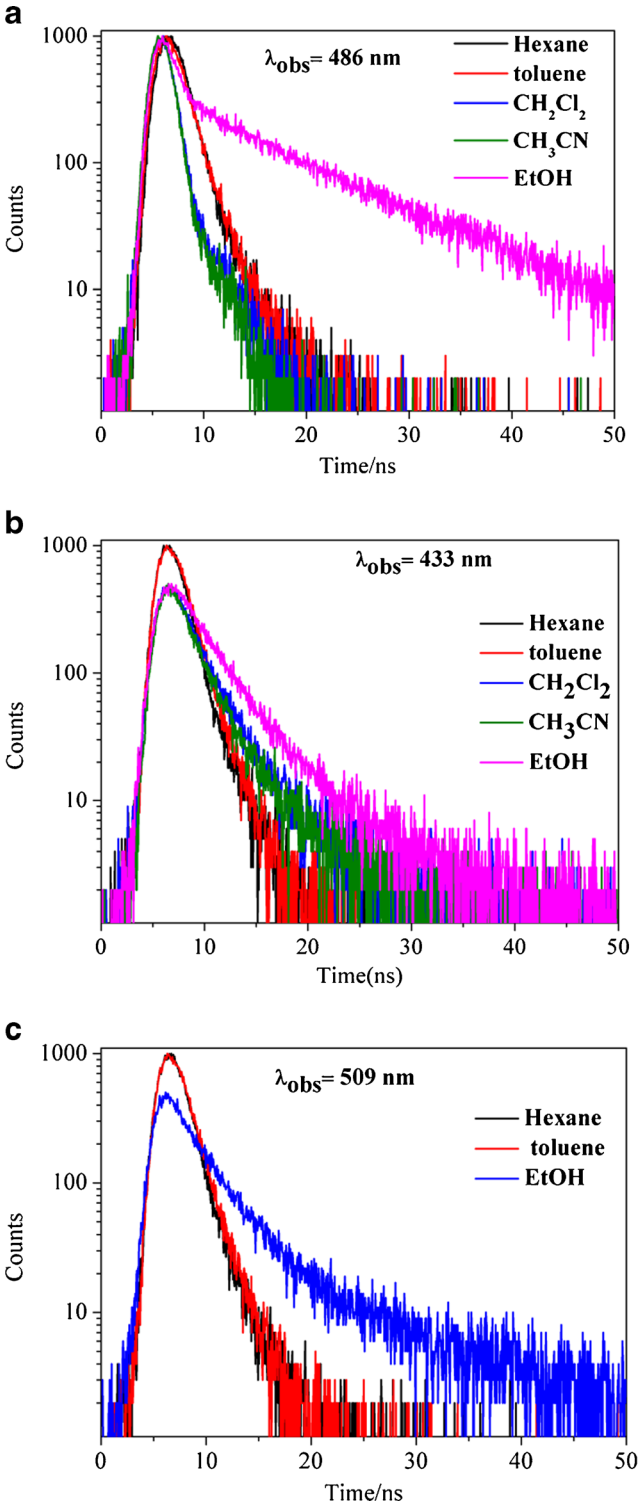

Fig. 4 Measured time-resolved fluorescence decays of (**a**)**1** and (**b** and **c**)**2** in different solvents from TCSPC data. The observation wavelength is indicated as insets. The sample was excited at 365 nm for **1** and at 350 nm for **2**

aromatic rings of the naphthalene moiety of the K form. Such a proton-transferred form (keto form) is not expected to be very stable. On the contrary, in compound **2**, the K form has a nodal plane through both aromatic rings of the naphthalene moiety, thus the energy of the K form of compound **2** is significantly lowered than that of **1**, resulting in a very large Stokes shift of **2**.

Picosecond Time-Resolved Fluorescence Study

To achieve a deeper insight into the photodynamics of the investigated compound **1** and **2**, we carried out a picosecond time-resolved study of the above solutions. Figure 4 showed the representative emission decays of compound **1** and **2** in used solvents measured at the emission wavelengths predominantly enol or keto isomers and upon excitation at 365 nm for **1** and at 350 nm for **2**. Corresponding fitting parameters were summarized in supplementary material Table S2. For **1**, The decays were fitted stimultaneously using a biexponential model except in toluene, which gave decay times of 0.90–1.69 and 3.66–11.31 ns, respectively. The trend showing the shortening of both fast and slow times with the polarity of the medium was clear, and was indicative of the involvement of an ICT process in excited **1** in polar solvents (CH_2Cl_2 and CH_3CN). The fluorescence decays of **2** presented a biexponential behavior with longer and shorter components in n-hexane and toluene. The shorter τ_1 (1.12–3.55 ns) were decaying at all of the observation wavelengths, and we assigned the component to decay of the normal excited state. The longer components τ_2(10.91, 17.29 ns) were considered as the decay of the normal/tautomer equilibrated excited state. It was found that in alcoholic solvent EtOH, the measured fluorescence decays of both **1** and **2** were different from other aprotic solvents which indicated that H-bonding interactions of the dyes with the medium were also involved in the process [26, 27].

Theoretical Calculation

DFT calculations were carried out under the effect of dichloromethane. Firstly, the ground state and the first excited state of **1** and **2** were optimized in the enol form and the keto form. It is to mention here that there were two different stable structures for 1 and 2 (Fig. 5) in the ground state. The calculated structures cartesian coordinates were listed in supplementary material scheme S3 and scheme S4. Theoretical calculations suggested that both (a) and (c) in either gas or organic solvents (CH_2Cl_2 and n-hexane) were more stable than (b) and (d), which could be attributed to the existence of the intramolecular O-H···N hydrogen bond. The detailed structural parameters were displayed in Table 1. For the case of **1**, it could be summarized as following: (1) the bond length of N3-C4 in E form was much shorter than that of K form, while the one of C9-O10 in E form was much longer than that of K form, which strongly suggested that both N3-C4 in E form and C9-O10 in K form had a double-bond characteristic. (2) In the comparison between E and E*, it was observed that N3 atom was pulled to C2 = O1 group and H11 atom was pulled to N3 atoms, resulting in the elongation of N3-C4 (c.a. 0.026 Å) and O10-H11 bonds (c. a. 0.066 Å). (3) In the K* form, N3 atom was pulled along the direction of N3-C6 and O10 atom was pulled away from C9 around 0.01 Å. And the N-H bond was only elongated a little. Interestingly, different to **1**, the K form of **2** is not stable, where the optimized structure of K

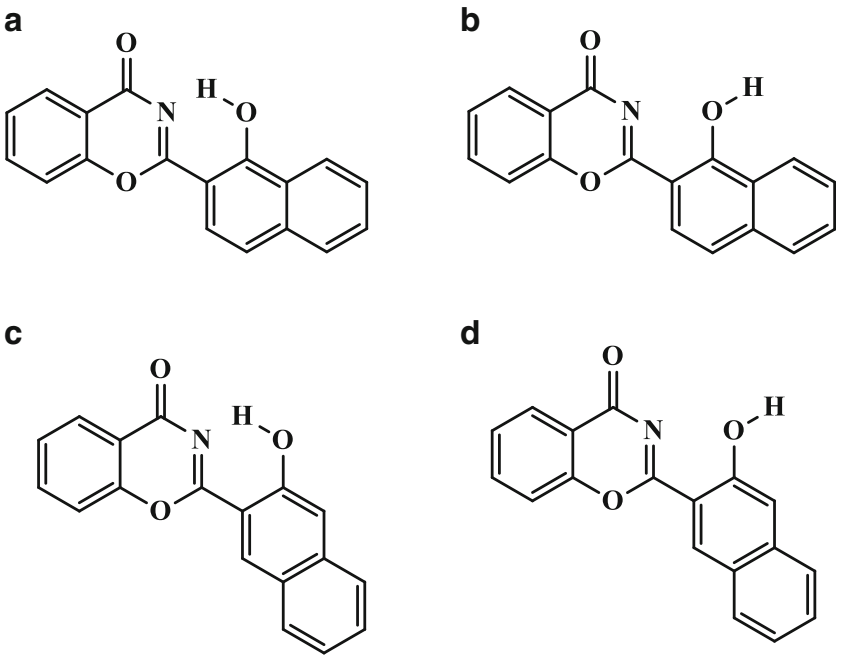

Fig. 5 Two stable enol-form structures of **1** (**a**–**b**) and **2** (**c**–**d**)

Table 1 Structural parameters for E, E*, K and K* of **1** and **2**

	1			
	E	E*	K	K*
R(C2-N3)	1.3980	1.3765	1.3899	1.3838
R(N3-C4)	1.2984	1.3248	1.3509	1.3474
R(C4-O5)	1.3499	1.3614	1.3445	1.3503
R(O5-C6)	1.3730	1.3718	1.3741	1.3735
R(C9-O10)	1.3229	1.3062	1.2502	1.2609
R(O10-H11)	1.0046	1.0709	-	-
R(N3-H11)	-	-	1.0467	1.0483
	2			
	E	E*	K	K*
R(C2-N3)	1.4031	1.3836	-	1.3826
R(N3-C4)	1.2904	1.3502	-	1.3490
R(C4-O5)	1.3501	1.3487	-	1.3486
R(O5-C6)	1.3728	1.3735	-	1.3738
R(C9-O10)	1.3367	1.2639	-	1.2652
R(O10-H11)	0.9906	-	-	-

form converted to E form. Surprisingly, the E* form is the K* form (Fig. 6).

UV-vis absorption and emission spectra were calculated in solvent of n-hexane. For 1, the obtained absorption peaks were at 327 nm for E → E* and at 370 nm for K → K*, comparable to the experimental values(294 nm for E → E* and 383 nm for K → K*). And the calculated emission peaks were 378 nm for E* → E and 425 nm for K* → K. Thus, the experimental emission peaks of 470 nm could be attributed to the transition of K* → K. For 2, the resulting theoretical absorption peaks were 333 nm for E → E*, being in good agreement with experimentally observed value(320 nm). And the obtained emission peak of 387 nm for E* → E was in good agreement with the first observed peaks (c.a. 420 nm).

The plots of the potential curves of internal proton transfer in S_0 and S_1 states of **1** and **2** as a function of O-H distance were performed and presented in Fig. 7. The barriers for tautomerization of the enol to the keto form were estimated. For **1**, there were two different stable states (d(O-H) = 1.0 and 1.65 Å) at the ground state, compatible with E and K forms. The energy barrier in E → K process was 18.5 kJ/mol and suggested that the proton transfer between them was so easy. Likewise two stable states (d(O-H) = 1.00 and 1.55 Å) in first existed state could be assigned to E* and K*. The resulting energy barriers were 16.0 kJ/mol for E* → K* and 5.0 kJ/mol for K* → E*, which can imply larger possibility of inter-transformation in the E* → K* and the K* → E* processes. However, inspecting the PES of **2**, we found two different curves from those of **1**. Both K and K* form in **2** are not stable. Thus, ESIPT process in **2** was very difficult. However, ESIPT behavior of **2** can be found in our experiment. This difference can be due to imperfect description of PCM-DFT methods in the solvent effect. It must to be mentioned here that the tunnel effect of the hydrogen atom should be existed, because it could lower the proton exchange barrier and even make the enthalpy barrier zero [28, 29].

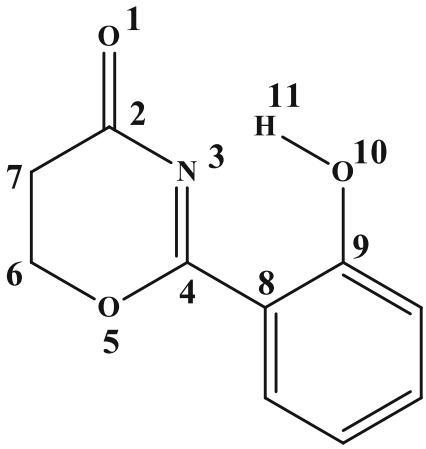

Fig. 6 The core part of **1** and **2**

Conclusions

In summary, two ESIPT molecules **1** and **2** were synthesized and studied, which have the similar structure but different luminescence characteristics. Experimental data demonstrated

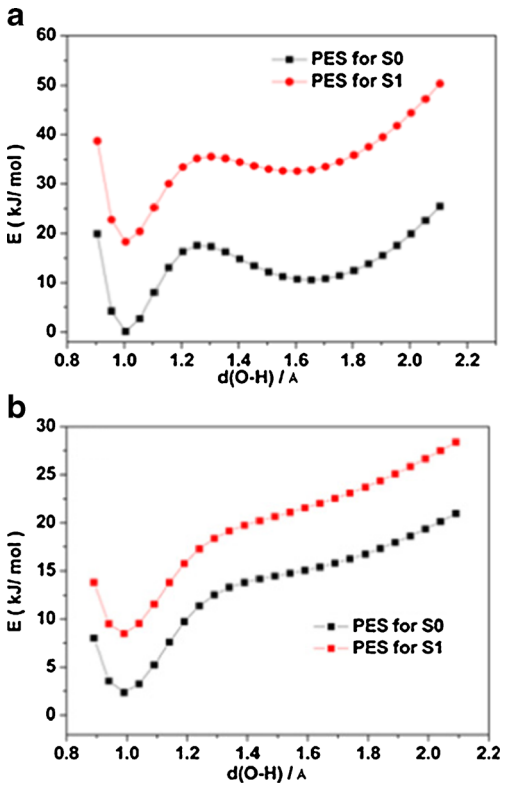

Fig. 7 Potential energy surface of proton transition in ground state and first exited state for (**a**) **1** and (**b**) **2**

that compound **1** would facilitate ESIPT process and favor the keto tautomer emission in various solvents, while compound **2** would suppress the ESIPT process and favor the enol emission in polar solvent. Theoretical studies indicated that there are two different stable structures for **1** and **2** in enol-form. DFT and PES of proton transition showed that both K and K* form in **2** are not stable compared with **1** and compound **1** was easier to undergo ESIPT. UV-vis absorption and emission spectra were also calculated and the results agreed well with the experimental values in some degree. Theoretical calculation for compound **1** and **2** verified our experimental data and allowed us to probe detailed mechanism analysis for the ESIPT reaction.

Acknowledgments The authors gratefully thank the support from International S&T Cooperation Program of China (2012DFA51210), National Natural Science Foundation of China (51203138, 51273179, 51573165), Natural Science Foundation of Zhejiang Province, China (LY15E030006) and Natural Science Foundation of Zhejiang University of Technology (1401101002408).

References

1. Abou-Zied OK, Jimenez R, Romesberg FE (2001) Tautomerization dynamics of a model base pair in DNA. J Am Chem Soc 123:4613–4614
2. Ray D, Paul BK, Guchhait N (2012) Effect of biological confinement on the photophysics and dynamics of a proton-transfer phototautomer: an exploration of excitation and emission wavelength-dependent photophysics of the protein-bound drug. Phys Chem Chem Phys 14:12182–12192
3. Lan X, Yang D, Sui X et al (2013) Time-dependent density functional theory (TD-DFT) study on the excited-state intramolecular proton transfer (ESIPT) in 2-hydroxybenzoyl compounds: significance of the intramolecular hydrogen bonding. Spectrochim Acta A 102:281–285
4. Zhao J, Ji S, Chen Y, Guo H, Yang P (2012) Excited state intramolecular proton transfer (ESIPT): from principal photophysics to the development of new chromophores and applications in fluorescent molecular probes and luminescent materials. Phys Chem Chem Phys 14:8803–8817
5. Kwon JE, Park SY (2011) Advanced organic optoelectronic materials: harnessing excited-state intramolecular proton transfer (ESIPT) process. Adv Mater 23:3615–3642
6. Paterson MJ, Robb MA, Blancafort L, DeBellis AD (2005) Mechanism of an exceptional class of photostabilizers: a seam of conical intersection parallel to excited state intramolecular proton transfer (ESIPT) in o-hydroxyphenyl-(1, 3, 5)-triazine. J Phys Chem A 109:7527–7537
7. Sun W, Li S, Hu R, Qian Y, Wang S, Yang G (2009) Understanding solvent effects on luminescent properties of a triple fluorescent ESIPT compound and application for white light emission. J Phys Chem A 113:5888–5895
8. Klymchenko AS, Shvadchak VV, Yushchenko DA, Jain N, Mély Y (2008) Excited-state intramolecular proton transfer distinguishes microenvironments in single-and double-stranded DNA. J Phys Chem B 112:12050–12055
9. Weller A (1961) Fast reactions of excited molecules. Prog React Kinet 1:187
10. Lamola AA, Sharp LJ (1966) Environmental effects on the excited states of o-hydroxy aromatic carbonyl compounds. J Phys Chem 70:2634–2638
11. Bader AN, Ariese F, Gooijer C (2002) Proton transfer in 3-hydroxyflavone studied by high-resolution 10 K laser-excited Shpol'skii spectroscopy. J Phys Chem A 106:2844–2849
12. Schmidtke SJ, Underwood DF, Blank DA (2004) Following the solvent directly during ultrafast excited state proton transfer. J Am Chem Soc 126:8620–8621
13. Douhal A, Amat-Guerri F, Acuna AU (1995) Photoinduced intramolecular proton transfer and charge redistribution in imidazopyridines. J Phys Chem 99:76–80
14. Piechowska J, Huttunen K, Wróbel Z, Lemmetyinen H, Tkachenko NV, Gryko DT (2012) Excited state intramolecular proton transfer in electron-rich and electron-poor derivatives of 10-Hydroxybenzo [h] quinoline. J Phys Chem A 116:9614–9620
15. Stasyuk AJ, Banasiewicz M, Cyrański MK, Gryko DT (2012) Imidazo [1, 2-a] pyridines susceptible to excited state intramolecular proton transfer: one-pot synthesis via an Ortoleva-King reaction. J Organomet Chem 77:5552–5558
16. Shigemitsu Y, Mutai T, Houjou H, Araki K (2012) Excited-state intramolecular proton transfer (ESIPT) emission of hydroxyphenylimidazopyridine: computational study on enhanced and polymorph-dependent luminescence in the solid state. J Phys Chem A 116:12041–12048
17. Wu Y, Peng X, Fan J, Gao S, Tian M, Zhao J, Sun S (2007) Fluorescence sensing of anions based on inhibition of excited-state intramolecular proton transfer. J Organomet Chem 72:62–70
18. Patil VS, Padalkar VS, Tathe AB, Gupta VD, Sekar N (2013) Synthesis, photo-physical and DFT studies of ESIPT inspired novel 2-(2′, 4′-dihydroxyphenyl) benzimidazole, benzoxazole and benzothiazole. J Fluoresc 23:1019–1029
19. Hadjoudis E, Mavridis IM (2004) Photochromism and thermochromism of Schiff bases in the solid state: structural aspects. Chem Soc Rev 33:579–588
20. Jakobsen P, Horneman AM, Persson E (2000) Inhibitors of the tissue factor/factor VIIa-induced coagulation: synthesis and in vitro evaluation of novel 2-aryl substituted pyrido [3, 4-d][1, 3]-, pyrido [2, 3-d][1, 3]-, pyrazino [2, 3-d][1, 3]-, pyrimido [4, 5-d][1, 3]-, pyrazolo [3, 4-d][1, 3]-, thieno [3, 2-d][1, 3]-and thieno [2, 3-d][1, 3]-oxazin-4-ones. Bioorg Med Chem 8:2803–2812
21. Geigy J. R. A.-G. 2-Substituted-phenyl-4H-1,3-benzoxazin-4-ones[P]. GB: 1152980, 1969 5 21.
22. Frisch MJ, Trucks GW, Schlegel HB, Scuseria GE, Robb MA, Cheeseman JR, Scalmani G, Barone V, Mennucci B, Petersson GA, Nakatsuji H, Caricato M, Li X, Hratchian HP, Izmaylov AF, Bloino J, Zheng G, Sonnenberg JL, Hada M, Ehara M, Toyota K, Fukuda R, Hasegawa J, Ishida M, Nakajima T, Honda Y, Kitao O, Nakai H, Vreven T, Montgomery JA, Jr., Peralta JE, Ogliaro F, Bearpark M, Heyd JJ, Brothers E, Kudin KN, Staroverov VN, Kobayashi R, Normand J, Raghavachari K, Rendell A, Burant JC, Iyengar SS, Tomasi J, Cossi M, Rega N, Millam JM, Klene M, Knox JE, Cross JB, Bakken V, Adamo C, Jaramillo J, Gomperts R, Stratmann RE, Yazyev O, Austin AJ, Cammi R, Pomelli C, Ochterski JW, Martin RL, Morokuma K, Zakrzewski VG, Voth GA, Salvador P, Dannenberg JJ, Dapprich S, Daniels AD, Farkas Ö, Foresman JB, Ortiz JV, Cioslowski J, and Fox DJ (2009) Gaussion 09 Revision A.1. Gaussian Inc, Wallingford
23. Gutierrez M, Alarcos N, Liras M, Sánchez F, Douhal A (2015) Switching to a reversible proton motion in a charge-transferred dye. J Phys Chem B 119:552–562
24. Nagaoka SI, Nagashima U (1989) Intramolecular proton transfer in various electronic states of o-hydroxybenzaldehyde. Chem Phys 136:153–163

25. Nagaoka SI, Kusunoki J, Fujibuchi T, Hatakenaka S, Mukai K, Nagashima U (1999) Nodal-plane model of the excited-state intramolecular proton transfer of 2-(o-hydroxyaryl) benzazoles. J Photochem Photobiol A Chem 122:151–159
26. Zhou P, Hoffmann MR, Han K, He G (2014) New insights into the dual fluorescence of methyl salicylate: effects of intermolecular hydrogen bonding and solvation. J Phys Chem B 119:2125–2131
27. Shynkar VV, Mely Y, Duportail G, Piémont E, Klymchenko AS, Demchenko AP (2003) Picosecond time-resolved fluorescence studies are consistent with reversible excited-state intramolecular proton transfer in 4'-(dialkylamino)-3-hydroxyflavones. J Phys Chem A 107:9522–9529
28. Borst DR, Roscioli JR, Pratt DW, Florio GM, Zwier TS, Müller A, Leutwyler S (2002) Hydrogen bonding and tunneling in the 2-pyridone· 2-hydroxypyridine dimer. Effect Electro Excitation Chem Phys 283:341–354
29. Tautermann CS, Voegele AF, Liedl KR (2003) The ground state tunneling splitting of the 2-pyridone· 2-hydroxypyridine dimer. Chem Phys 292:47–52